RESEARCH ARTICLE
Cytoskeleton, March 2015 72:146–156 (doi: 10.1002/cm.21211)

Afadin Regulates RhoA/Rho-Associated Protein Kinase Signaling to Control Formation of Actin Stress Fibers in Kidney Podocytes

Koji Saito,[1] Tatsuhiro Shiino,[1] Hidetake Kurihara,[2] Yutaka Harita,[3] Seisuke Hattori[4] and Yasutaka Ohta[1]*

[1]Division of Cell Biology, Department of Biosciences, School of Science, Kitasato University, Kanagawa, Japan
[2]Department of Anatomy, School of Medicine, Juntendo University, Tokyo, Japan
[3]Department of Pediatrics, Graduate School of Medicine, University of Tokyo, Tokyo, Japan
[4]Division of Biochemistry, School of Pharmaceutical Sciences, Kitasato University, Tokyo, Japan

Received 22 July 2014; Revised 19 January 2015; Accepted 20 February 2015
Monitoring Editor: Makoto Kinoshita

The function of kidney podocytes is closely associated with actin cytoskeleton. Rho family small GTPase RhoA promotes stress fiber assembly through Rho-associated protein kinase (ROCK)-dependent myosin II phosphorylation and plays an important role in maintenance of actin stress fibers of podocytes. However, little is known how stress fiber assembly is regulated in podocytes. Here, we found that afadin, an actin filament-binding protein, is required for RhoA/ROCK-dependent formation of actin stress fibers in rat podocyte C7 cells. We show that depletion of afadin in C7 cells induced loss of actin stress fibers. Conversely, forced expression of afadin increased the formation of actin stress fibers. Depletion of afadin inactivated RhoA and reduced the phosphorylation of myosin II. Moreover, the DIL domain of afadin appears to be responsible for actin stress fiber formation. Thus, afadin mediates RhoA/ROCK signaling and contributes to the formation of actin stress fibers in podocyte cells. © 2015 Wiley Periodicals, Inc.

Key Words: afadin; Rho family small GTPase; RhoA/ROCK; actin stress fiber; podocyte

Introduction

Differentiated podocytes are specialized epithelial cells that possess actin-rich projections known as foot processes to cover the glomerular capillary loops [Faul et al., 2007]. Formation and maintenance of foot process is dependent on the polymerization and bundling of actin filaments. Disruption of the podocyte cell–cell junction and flattening of the process, so called foot process effacement, is induced by reorganization of actin filaments. Stress fibers are contractile actomyosin bundles found in many non-muscle cells [Pellegrin and Mellor, 2007] and often associated with actin cables that span along the foot processes [Kistler et al., 2012; Reiser and Sever, 2013]. Several actin-binding proteins such as α-actinin-4 [Weins et al., 2007], talin1 [Tian et al., 2014], and synaptopodin [Asanuma et al., 2006] have been implicated in regulation of stress fiber assembly and linked to proteinuric diseases [Mundel and Reiser, 2010]. Thus, podocyte actin cytoskeleton is critically involved in podocyte functions [Ichimura et al., 2003; Faul et al., 2007; Schlondorff, 2008].

Rho family small GTPases are master regulators of actin cytoskeletal dynamics [Jaffe and Hall, 2005]. RhoA induces stress fiber formation and Rac and Cdc42 are responsible for formation of protrusive structures including lamellipod and filopod. Rho small GTPases in podocytes have been shown to be critically involved in glomerular diseases [Mundel and Reiser, 2010; Mouawad et al., 2013; New et al., 2014]. Thus, maintenance of actin stress fibers and induction of motility of podocytes are dependent on activation and inactivation of Rho small GTPases [Kistler et al., 2012; Reiser and Sever, 2013].

Afadin (also called AF-6) is a filamentous actin (F-actin)-binding protein and binds along the sides of F-actin but does not have crosslinking activity [Mandai et al., 1997]. Afadin functions as an adaptor protein by binding to many scaffolds and F-actin-binding proteins through its multiple domains and contributes to the formation of a variety of cell–cell junctions [Takai et al., 2008]. In addition, afadin regulates cell morphology and migration thorough regulating small GTPase Rap1, Rac, and RhoA [Miyata et al., 2009; Fukumoto et al., 2011; Majima et al., 2013]. However, little is known if afadin is involved in the regulation of podocyte functions.

*Address Correspondence to: Yasutaka Ohta, Division of Cell Biology, Department of Biosciences, School of Science, Kitasato University, 1-15-1 Kitasato, Sagamihara, Minami-ku, Kanagawa 252-0373, Japan. E-mail: yohta@kitasato-u.ac.jp
Published online 25 February 2015 in Wiley Online Library (wileyonlinelibrary.com).

In this study, we showed that afadin is required for the formation of actin stress fibers in rat podocyte C7 cells. We present evidences that afadin controls actin stress fiber formation by regulating RhoA/ROCK signaling.

Results

Afadin Is Required for RhoA/ROCK-Dependent Formation of Actin Stress Fibers in Rat Podocyte C7 Cells

To investigate whether afadin could regulate actin cytoskeleton in podocyte cells, we used C7 cells in this study. C7 cells were originally isolated as kidney podocyte cells from decapsulated glomeruli of tsA58 transgenic rats as described previously [Eto et al., 2007]. The temperature-sensitive cells were cultured and grown at the permissive temperature of 33°C, and were then shifted to the nonpermissive temperature of 37°C to induce differentiation (Fig. 1A). The differentiated C7 cells spread and exhibit long processes (Figs. 1A and 1B) and abundant actin stress-fiber structures stained with phalloidin in the cell bodies (Fig. 1C), as seen in other cultured podocytes [Chittiprol et al., 2011]. In this study, we analyzed differentiated C7 cells that were cultured at 37°C for 7 days. We first transfected C7 cells with small interference RNAs (siRNAs) targeting *afadin*. Two-independent siRNAs targeting *afadin* (KD#1 and KD#2) reduced the expression of endogenous afadin in C7 cells (Fig. 1D). Depletion of afadin by siRNAs remarkably reduced long processes and stress-fiber structures in the cell bodies (Figs. 1B and 1C). Depletion of afadin also caused the formation of F-actin-rich rim around cell peripheries (Fig. 1C). We quantified the density of stress fibers, along a line across the cell as shown in Fig. 1E, and the data are summarized in Fig. 1F. Afadin depletion resulted in a significant decrease of stress fiber density in the cell body. Conversely, overexpression of GFP-tagged afadin increased stress fibers in the cytoplasm (Fig. 1G) and elicited a significant increase of stress fiber density (Fig. 1H).

Maintenance of actin stress fibers is dependent on activation of RhoA in podocytes [Kistler et al., 2012; Reiser and Sever, 2013]. Indeed, RhoA inactivation has been shown to induce loss of actin stress fibers in podocytes [Asanuma et al., 2006; Tian et al., 2010; Wang et al., 2012]. The formation of stress fibers observed in C7 cells was also dependent on RhoA/ROCK and myosin. Depletion of RhoA by siRNAs (KD#1 and KD#2) reduced the expression of endogenous RhoA (Fig. 2A) and decreased stress fibers (Figs. 2B and 2C). Treatment of C7 cells with a ROCK-specific inhibitor Y27632 induced cell morphologies very similar to those of RhoA-depleted cells and decreased stress fibers (Figs. 2D and 2E). Similarly, treatment of C7 cells with a Myosin II inhibitor blebbistatin also abolished stress fibers throughout the cytoplasm (Figs. 2D and 2E). Thus, our results showed that afadin is required for RhoA/ROCK-dependent formation of actin stress fibers in C7 podocyte cells.

Afadin Regulates RhoA/ROCK Signaling and Induces Actin Stress Fibers

We next examined whether loss of actin stress fibers in afadin-depleted C7 cells was caused by decreased RhoA/ROCK/myosin activities. Depletion of afadin significantly reduced GTP-bound RhoA as shown by Rhotekin-RBD pull-down assay (Fig. 3A). Previous study showed that depletion of afadin in mouse fibroblast NIH3T3 cells increases GTP-bound RhoA [Miyata et al., 2009], suggesting that the inactivation of RhoA in afadin-depleted C7 cells may be cell context-dependent. In our pull-down assay, however, afadin depletion in NIH3T3 cells did not increase GTP-bound RhoA (Fig. 3A) but importantly, did not reduce GTP-bound RhoA as observed in C7 cells.

Consistent with the downregulation of RhoA activity induced by afadin depletion in C7 cells, the phosphorylation of myosin light chain (MLC) was significantly reduced in afadin-depleted C7 cells (Fig. 3B). On the other hand, in PAK1-PBD pull-down assay, no differences were observed in the amount of active Rac1 and Cdc42 between control and afadin-depleted C7 cells (Fig. 3C), indicating that depletion of afadin does not affect the activation of Rac1 and Cdc42. Furthermore, we showed that the expression of constitutively active Rho G14V mutant rescued the loss of actin stress fibers induced by afadin depletion (Figs. 4A and 4B), whereas overexpression of GFP-afadin did not rescue the loss of actin stress fibers in RhoA-depleted cells (Figs. 4C and 4D). These results suggest that afadin is required for RhoA activity and formation of actin stress fibers in C7 cells.

Identification of Afadin Domains Mediating Actin Stress Fiber Formation

Afadin is an adaptor protein that has multiple domains (Fig. 5A) and binds to a variety of proteins [Takai et al., 2008]: the RA domain binds to Rap1, a member of the Ras family of small GTPases; the DIL domain binds to afadin DIL-domain-interacting protein (ADIP); the PDZ domain binds to many proteins including transmembrane protein nectin and Spa1, a Rap1 GAP; the FAB domain binds to F-actin. To determine which domain of afadin is responsible for actin stress fiber formation, we transfected C7 cells with a GFP-afadin mutant lacking RA domain (ΔRA), DIL domain (ΔDIL), PDZ domain (ΔPDZ), or FAB domain (ΔFAB) [Nakata et al., 2007], and quantified the density of stress fibers at the cell cytoplasm. We confirmed that each mutant protein was expressed equally well by immunoblotting in HEK293 cells (Fig. 5B). We found that overexpression of GFP-afadin ΔDIL mutant in C7 cells decreased actin stress fibers in the cell bodies and caused the formation of F-actin-rich rim around cell peripheries (Fig. 5C),

similar to the cell morphologies induced by afadin depletion. Consistently, the density of stress fibers was significantly decreased by GFP-afadin ΔDIL mutant (Fig. 5D). Therefore, GFP-afadin ΔDIL mutant seems to function as a dominant-negative inhibitor of endogenous afadin that induces actin stress fibers through its DIL domain.

It has been shown that Rap1 binds to the RA domain of afadin and modulates RhoA activity to control actin-cytoskeletal reorganization of migrating and endothelial cells [Miyata et al., 2009; Birukova et al., 2013]. However, overexpression of GFP-afadin ΔRA mutant, which lacks both RA1 and RA2 domains and can not bind to Rap1 [Boettner et al., 2003; Hoshino et al., 2005], did not decrease stress fibers, nor did it affect cell morphology in C7 cells (Figs. 5C and 5D). In addition, depletion of Rap1 by siRNAs (KD#1 and KD#2) did not affect stress fiber

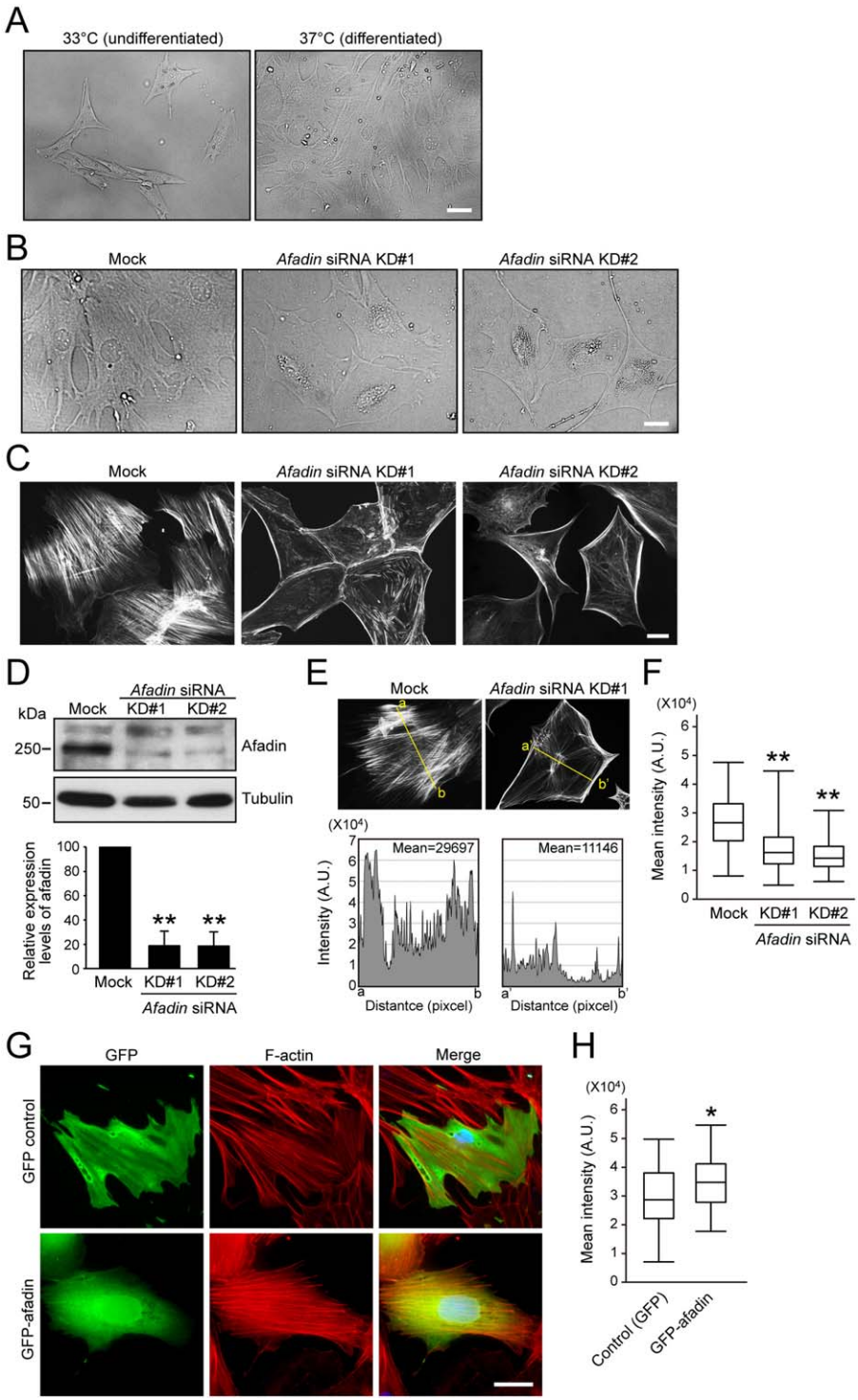

Fig. 1.

formation in control C7 cells (Figs. 6A– 6C), and in C7 cells transfected with afadin (Figs. 6D and 6E). Finally, no difference was observed in the amount of active Rap1 between control and afadin-depleted C7 cells as determined by RalGDS-RBD pull-down assay (Fig. 6F). These data suggest that afadin could modulate RhoA activity through a Rap1-independent pathway in C7 cells. GFP-afadin ΔPDZ or ΔFAB-overexpressing cells, as well as GFP-afadin full-length-overexpressing cells, elicited a significant increase of stress fiber density (Figs. 5C and 5D). Therefore, our results suggest that afadin may be required for RhoA activity through its DIL domain to induce actin stress fibers in C7 cells.

Discussion

In this study, we demonstrated that afadin plays a critical role in actin stress fiber formation in rat podocyte C7 cells. Stress fibers play a central role in cell adhesion and morphogenesis, and RhoA/ROCK signaling regulates its assembly [Pellegrin and Mellor, 2007]. We showed that afadin controls the formation of actin stress fibers by regulating RhoA/ROCK signaling in C7 cells. First, depletion of afadin induced loss of actin stress fibers, whereas overexpression of afadin increased its formation. Second, depletion of afadin inactivated RhoA and reduced the phosphorylation of MLC. Third, RhoA appears to be located downstream of afadin, because constitutively active RhoA G14V mutant could rescue the loss of actin stress fibers induced by afadin depletion but forced expression of afadin did not rescue the loss of actin stress fibers in RhoA-depleted cells. Thus, afadin appears to be required for RhoA activity and RhoA/ROCK-dependent formation of actin stress fibers in C7 cells.

RhoA plays an important role in modulating the integrity of podocyte cytoskeleton under basal conditions [Kistler et al., 2012; Reiser and Sever, 2013]. Imbalance of RhoA activity causes podocyte injury and proteinuria [Zhu et al., 2011; Wang et al., 2012]. In cultured podocytes, RhoA inactivation induces loss of actin stress fibers and its hyperactivation induces more stress fibers [Asanuma et al., 2006; Tian et al., 2010; Wang et al., 2012]. In addition, mutations or deletion of *MYH9* gene, which encodes myosin II, cause a variety of glomerular diseases [Singh et al., 2009; Johnstone et al., 2011]. In cultured podocytes, knockdown of myosin II induces loss of stress fibers [Hays et al., 2014], and stress fiber formation is associated with RhoA-dependent phosphorylation of MLC [Lal et al., 2014]. Stress fibers observed in cultured podocytes have been considered to represent healthy actin organization [Mundel et al., 2010], but there is no definite evidence that the stress fiber correlates with the normal actin structure in vivo [Mouawad et al., 1997]. Nevertheless, our present study suggests that afadin may play an important role in the regulation of podocyte actin cytoskeleton through the modulation of RhoA/ROCK/myosin signaling.

Our present study suggests that requirement of afadin for RhoA activity may be cell context-dependent. Depletion of afadin in C7 cell reduced GTP-bound RhoA. Previous study showed that depletion of afadin in mouse fibroblast NIH3T3 cells increases GTP-bound RhoA [Miyata et al., 2009]. Our study showed that depletion of afadin in NIH3T3 cells did not reduce nor increase GTP-RhoA. This discrepancy with the previous report might be explained by the difference of experimental conditions between the present and previous studies; in the previous report, afadin was stably depleted using shRNA, and the afadin-knockdown stable NIH3T3 cell line was cultured on vitronectin-coated dishes 16 h before the assay, while in our study, the cells were transiently transfected with *afadin* siRNA and cultured on noncoated dishes until the assay. Nonetheless, depletion of afadin reduced RhoA activity in C7 cells, but not in NIH3T3 cells in our study, suggesting the cell-type specific regulation of RhoA by afadin.

Fig. 1. Afadin is required for formation of actin stress fibers in C7 cells. A: C7 cells were cultured at the permissive temperature (33°C) and differentiated for 7 days at nonpermissive temperature (37°C). Differential interference contrast (DIC) images of undifferentiated (left) and differentiated (right) cells are shown. Scale bar, 100 μm. **B**: C7 cells cultured at 33°C were transfected with control (mock) or *afadin* siRNAs and cultured at 37°C for 7 d. DIC images of mock and afadin-depleted cells are shown. Scale bar, 50 μm. **C**: Mock and afadin-depleted cells cultured as in B were fixed and stained with phalloidin for F-actin. Scale bar, 50 μm. **D**: Depletion of afadin after 7 d of siRNA treatment was confirmed by immunoblotting using anti-afadin and anti-tubulin (loading control) antibodies. The signal intensity of the bands was quantified by ImageJ program. Data are presented as percentage of the expression level of mock cells. The expression level of afadin was normalized to that of tubulin and expressed as the means ± S.D. of three independent experiments. *P* values in comparison to mock cells as determined by Student's *t*-test are shown (**$P < 0.01$). **E**: Representative images of mock and afadin-depleted cells stained with phalloidin (above) and fluorescence intensities of F-actin across the lines shown in the corresponding cells (below). The *x*-axis represents distance (pixel) across the cell, and the *y*-axis represents levels of fluorescence intensity. Mean intensity is total intensity divided by number of pixels. **F**: Quantification of stress fiber density of mock and afadin-depleted cells. Mean intensities are shown as box and whisker plots. Median, quartiles, and highest and lowest values are indicated on box and whisker plots. More than 100 cells were analyzed, and *P* values in comparison to mock cells as determined by Mann–Whitney's *U*-test were shown (**$P < 0.01$). **G**: C7 cells that were cultured at 37°C for 6 d were transfected with a control plasmid (pEGFP) or pEGFP plasmid encoding afadin, followed by additional 24 h culture. The transfected cells were fixed and stained with anti-GFP antibody (green), phalloidin (red), and hoechst 33258 for nuclei (blue). Merged fluorescent images are shown. Scale bar, 50 μm. **H**: Quantification of stress fiber density of control (GFP) and GFP-afadin-overexpressing cells. Mean intensities were quantified as in E and shown as box and whisker plots as in F. The data of more than 40 transfected cells was statistically analyzed as in F (*$P < 0.05$).

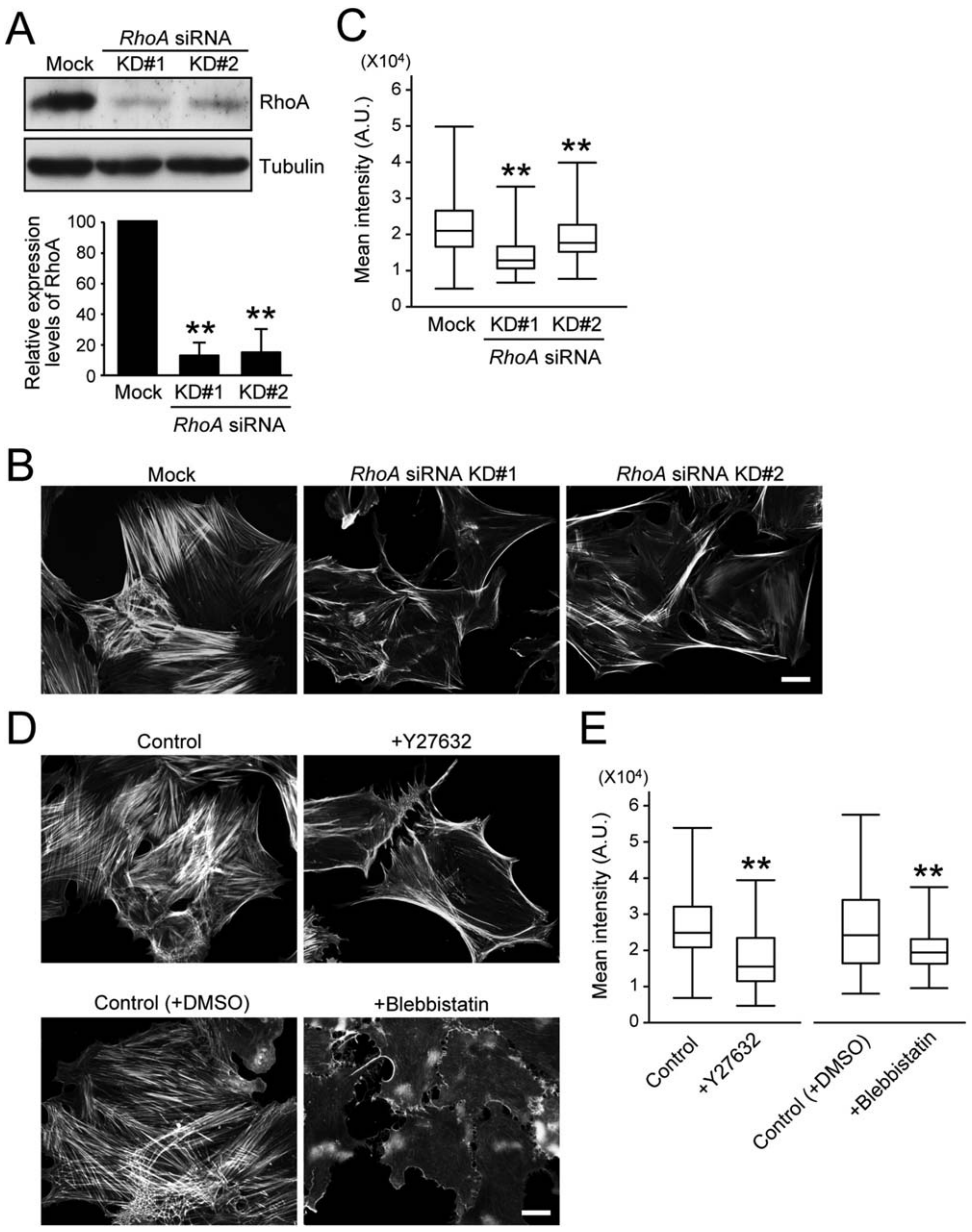

Fig. 2. RhoA/ROCK signaling mediates stress fiber formation in C7 cells. A: C7 cells cultured at 33°C were transfected with control (mock) or *RhoA* siRNAs and cultured at 37°C for 7 d. RhoA and tubulin (loading control) were detected by immunoblotting using anti-RhoA and anti-tubulin antibodies, respectively. The efficiency of RhoA depletion by siRNAs was quantified and statistically analyzed as in Fig. 1D (**$P < 0.01$). **B**: Mock and RhoA-depleted cells cultured as in A were fixed and stained with phalloidin for F-actin. Scale bar, 50 μm. **C**: Quantification of stress fiber density of mock and RhoA-depleted cells. The data of more than 100 cells was statistically analyzed as in Fig. 1F (**$P < 0.01$). **D**: For inhibition of ROCK or myosin II, C7 cells that were cultured at 37°C for 7 d were treated with 50 μM Y27632 for 4 h or 100 μM blebbistatin for 1 h, respectively. The treated cells were fixed and stained with phalloidin. Cells were also treated with DMSO as a control of blebbistatin. Scale bar, 50 μm. **E**: Quantification of stress fiber density of Y27632- and blebbistatin-treated cells. The data of more than 100 cells was statistically analyzed as in Fig. 1F (**$P < 0.01$).

How afadin regulates RhoA activity in podocyte cells is unclear. Previous studies have reported that afadin downregulates RhoA activity through its RA domain to modulate Rap1 in migrating and endothelial cells [Miyata et al., 2009; Birukova et al., 2013]. However, our result suggested that afadin regulates RhoA activity in a Rap1-independent manner in C7 cells. The afadin ΔRA mutant or Rap1 depletion had no effect on the formation of actin stress fibers in C7 cells, and overexpression of afadin increased stress fibers even in the Rap1-depleted cells. In addition, afadin depletion did not change the amount of active Rap1 in C7 cells. This Rap1-independent regulation of RhoA by afadin may be cell context-dependent.

Interestingly, overexpression of afadin ΔDIL mutant decreased actin stress fibers in C7 cells, suggesting that afadin may regulate RhoA activity through its DIL domain.

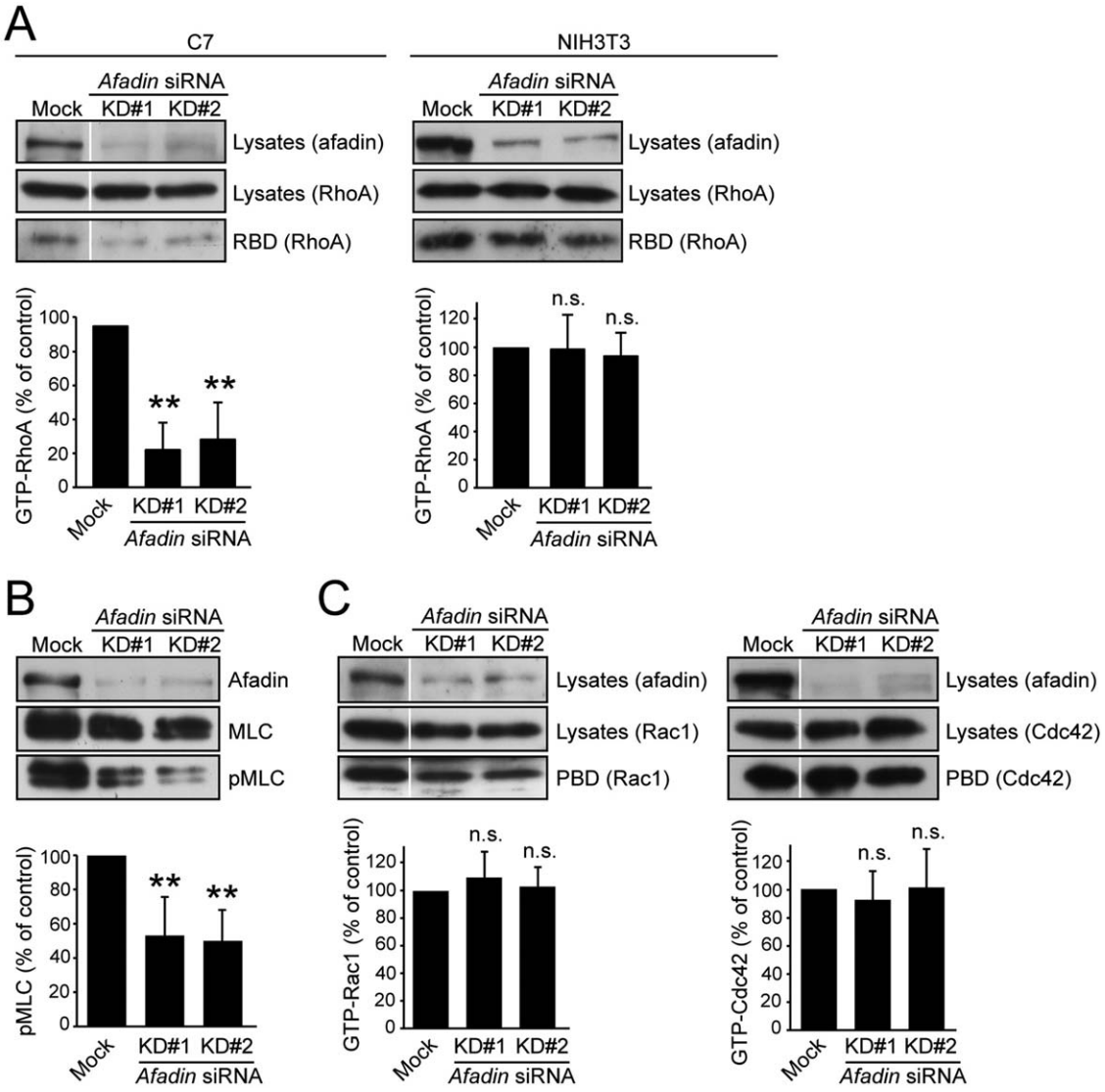

Fig. 3. Afadin modulates RhoA/ROCK activity in C7 cells. A: C7 cells cultured at 33°C were transfected with control (mock) or *afadin* siRNAs and cultured for 7 d. NIH3T3 cells were transfected with mock or *afadin* siRNAs for 48 h. Cell lysates were incubated with GST-Rhotekin-RBD that was immobilized on glutathione-Sepharose beads. The amount of RhoA in cell lysates before pull-down and GTP- (GST-RBD bound) RhoA was detected by immunoblotting using anti-RhoA antibody. Samples from C7 cells were run on the same gels. The signal intensity of the bands was quantified by ImageJ program. Depletion of afadin by siRNAs was confirmed by immunoblotting using anti-afadin antibody. The efficiency of afadin depletion by siRNAs in NIH3T3 cells was >80% measured by immunoblotting (data not shown). The amount of GTP-RhoA was normalized to that of total RhoA and expressed as the means ± S.D. of six (C7) or eight (NIH3T3) independent experiments. *P* values in comparison to control cells as determined by Student's *t*-test are shown (**$P < 0.01$; n.s. = not significant). **B**: C7 cells were transfected as in A. Afadin, MLC, and pMLC were detected by immunoblotting using anti-afadin, anti-MLC, and anti-pMLC, antibodies, respectively. The amount of pMLC was normalized to that of total MLC and expressed as the means ± S.D. of three independent experiments. The data was analyzed statistically as in A (**$P < 0.01$). **C**: C7 cells were transfected as in A. Cell lysates were incubated with GST-PAK1-PBD that was immobilized on glutathione-Sepharose beads. The amount of Rac1 or Cdc42 in cell lysates before pull-down and GTP- (GST-PBD bound) Rac1 or Cdc42 was detected by immunoblotting using anti-Rac or anti-Cdc42 antibody. Samples were run on the same gels. The amount of GTP-Rac1 or Cdc42 was normalized to that of total Rac1 or Cdc42 and expressed as the means ± S.D. of four independent experiments. The data was analyzed statistically as in A (n.s. = not significant).

Presumably, the afadin ΔDIL mutant acts as a dominant-negative mutant by displacing endogenous afadin that induces actin stress fibers through its DIL domain. The DIL domain has been found in afadin and type V myosins [Ponting, 1995]. The function of the DIL domain remains unknown but could be involved in protein–protein interaction [Böhl et al., 2000; Long et al., 2000; Fukumoto et al., 2011]. To date ADIP is the only identified protein that binds to the DIL domain of afadin [Asada et al., 2003]. ADIP plays essential roles in adherens junction formation through the interaction with cross-linking protein α-actinin [Asada et al., 2003] and in cell migration through the interaction with Rac

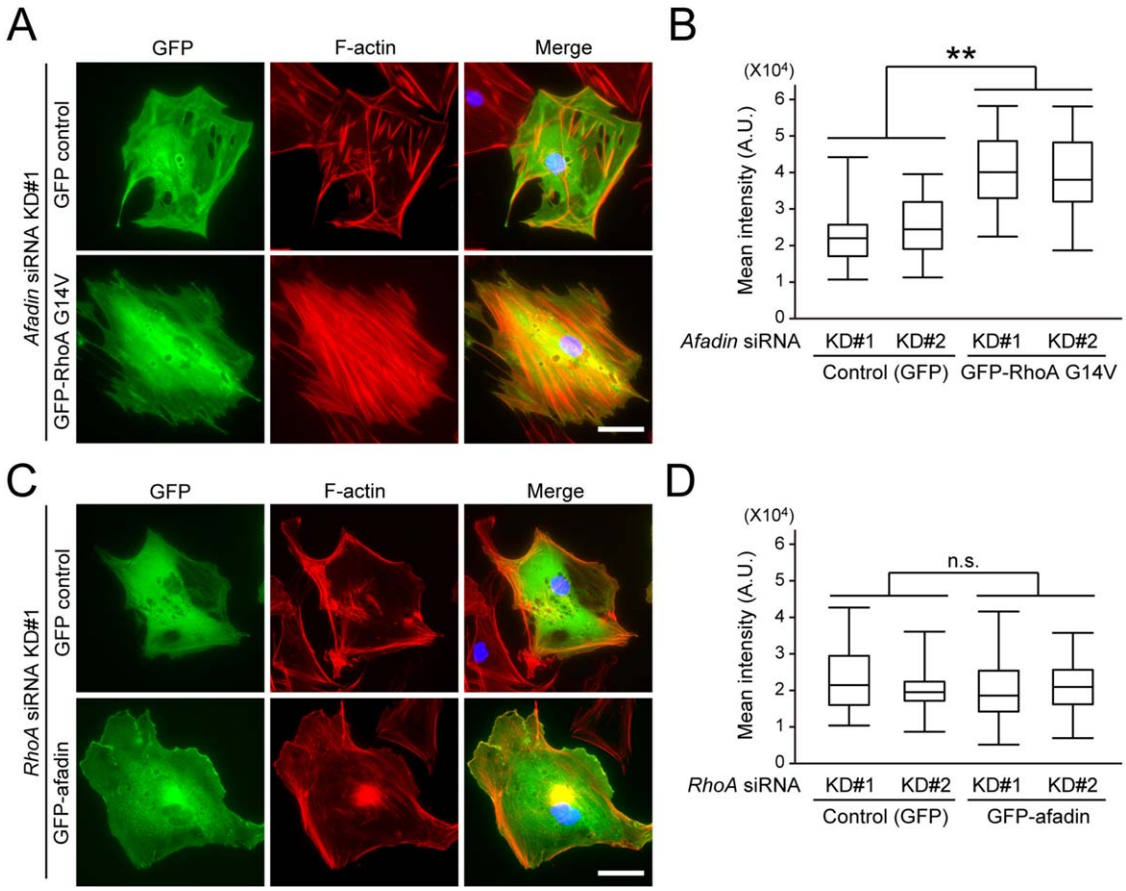

Fig. 4. Afadin induces actin stress fibers through RhoA in C7 cells. A: For cotransfection of plasmid DNA and siRNA, C7 cells cultured at 33°C were first transfected with *afadin* siRNAs and cultured at 37°C. After 6 d, cells were cotransfected with a control plasmid (pEGFP) or pEGFP plasmid encoding RhoA G14V, followed by additional 24 h culture. The cotransfected cells were fixed and stained with anti-GFP antibody (green), phalloidin for F-actin (red), and hoechst 33258 for nuclei (blue). Merged fluorescent images are shown. Scale bar, 50 μm. **B**: Quantification of stress fiber density of cells transfected as in A. The data of more than 40 transfected cells was analyzed statistically as in Fig. 1F (**$P < 0.01$). **C**: Cotransfection of pEGFP plasmid encoding afadin and *RhoA* siRNAs was performed as in A. The cotransfected cells were fixed and stained as in A. Merged fluorescent images are shown. Scale bar, 50 μm. **D**: Quantification of stress fiber density of cells transfected as in C. The data of more than 40 transfected cells was analyzed statistically as in Fig. 1F (n.s. = not significant).

GEF Vav2 [Fukumoto et al., 2011]. ADIP also binds to β'-COP, a subunit of the coatomer complex, and localizes at the Golgi complex [Asada et al., 2004], suggesting the involvement of ADIP in membrane trafficking. We could not detect interaction between endogenous afadin and ADIP by immunoprecipitation with anti-afadin antibody in C7 cells (data not shown). It is therefore unclear if afadin binds to ADIP and modulate RhoA activity in C7 cells. Further study is required to determine the role of the DIL domain of afadin in actin stress fiber formation.

In conclusion, we first demonstrated a role of afadin in organization of actin cytoskeleton of podocyte cells. Afadin is required for RhoA activity and RhoA/ROCK-dependent actin stress fiber formation. Afadin seems to induce RhoA-dependent actin stress fibers to maintain actin cytoskeletal integrity of podocyte cells. It will be important to determine if afadin is responsible for maintaining the filtration barrier of kidney glomerulus.

Materials and Methods

Reagents

The pEGFP-c1 plasmid (Clontech, Palo Alto, CA) encoding afadin constructs (full length, ΔRA, ΔDIL, ΔPDZ, and ΔFAB) [Nakata et al., 2007] was a gift from Y. Takai (Kobe University, Japan). The pEGFP-RhoA G14V plasmid was generated as follows; the RhoA G14V coding sequence was PCR-amplified using pCMV5-Myc-based plasmid as a template and the PCR products were inserted into the pEGFP-c1 vector and sequenced. Rabbit anti-afadin and anti-GFP polyclonal antibodies were purchased from Sigma (St. Louis, MO) and MBL (Nagoya, Japan), respectively. Mouse anti-pMLC (Ser19) and anti-RhoA monoclonal antibodies were purchased from Santa Cruz Biotechnology (Santa Cruz, CA). Mouse anti-Cdc42 and anti-Rap1 monoclonal antibodies were purchased from BD Biosciences (Bedford, MA). Mouse anti-α-tubulin and anti-Rac1

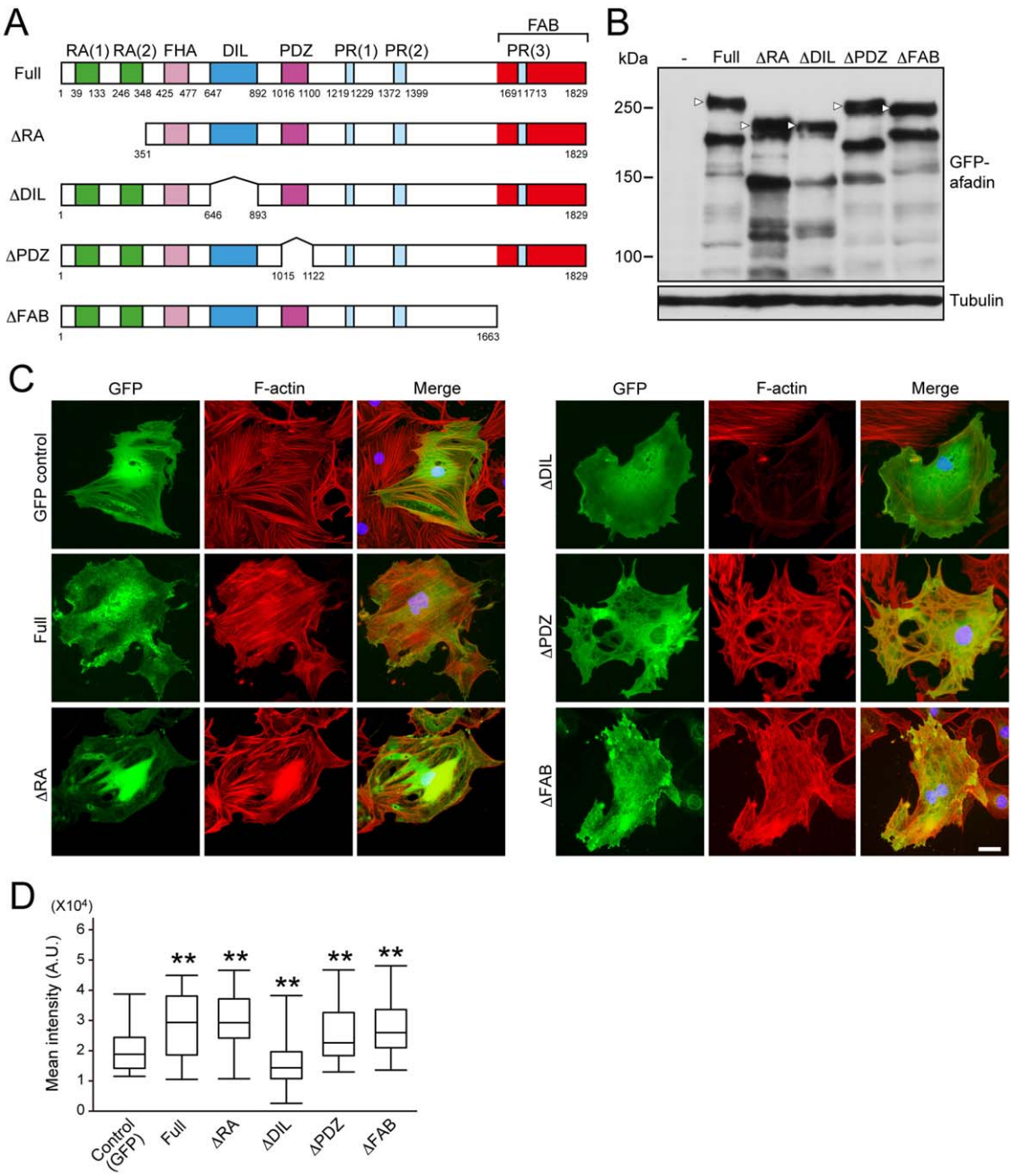

Fig. 5. DIL domain of afadin appears to be responsible for actin stress fiber formation in C7 cells. A: Schematic diagram of rat afadin constructs. RA, Ras-associated domain; FHA, forkhead-associated domain; DIL, dilute domain; PDZ, PDZ domain; PR, proline-rich domain; FAB, F-actin-binding domain. **B**: Ectopic expression of GFP-afadin constructs. HEK293 cells were transfected without (-) or with GFP-afadin constructs. GFP-afadin proteins were analyzed by immunoblotting using anti-GFP antibody. Tubulin was used as a loading control. **C**: C7 cells that were cultured at 37°C for 6 d were transfected with a control plasmid (pEGFP) or pEGFP plasmid encoding afadin constructs (full length, ΔRA, ΔDIL, ΔPDZ, and ΔFAB), followed by additional 24 h culture. The transfected cells were fixed and stained with anti-GFP antibody (green), phalloidin for F-actin (red), and hoechst 33258 for nuclei (blue). Merged fluorescent images are shown. Scale bar, 50 μm. **D**: Quantification of stress fiber density of cells transfected as in C. The data of more than 40 transfected cells was analyzed statistically as in Fig. 1F (**$P < 0.01$). [Color figure can be viewed in the online issue, which is available at wileyonlinelibrary.com.]

monoclonal antibodies were purchased from Sigma and Millipore (Billerica, MA), respectively. Secondary antibodies conjugated to Alexa Fluor 488 or 568 or Alexa Fluor 568-phalloidin (Invitrogen, Carlsbad, CA); hoechst 33258 (Dojindo laboratories, Kumamoto, Japan); Y27632 or blebbistatin (Sigma) were also purchased from commercial sources.

siRNA

siRNA oligonucleotide duplexes targeting *afadin*, *RhoA*, and *Rap1* were purchased from Invitrogen. The targeting sequences were as follows: *afadin*, KD#1 5'-GAGAAACC UCUAGUUGUACAGUUGA-3' (rat and mouse, nt 322–346) and KD#2 5'-CAUGGAUCGCAAGUGUGACAG

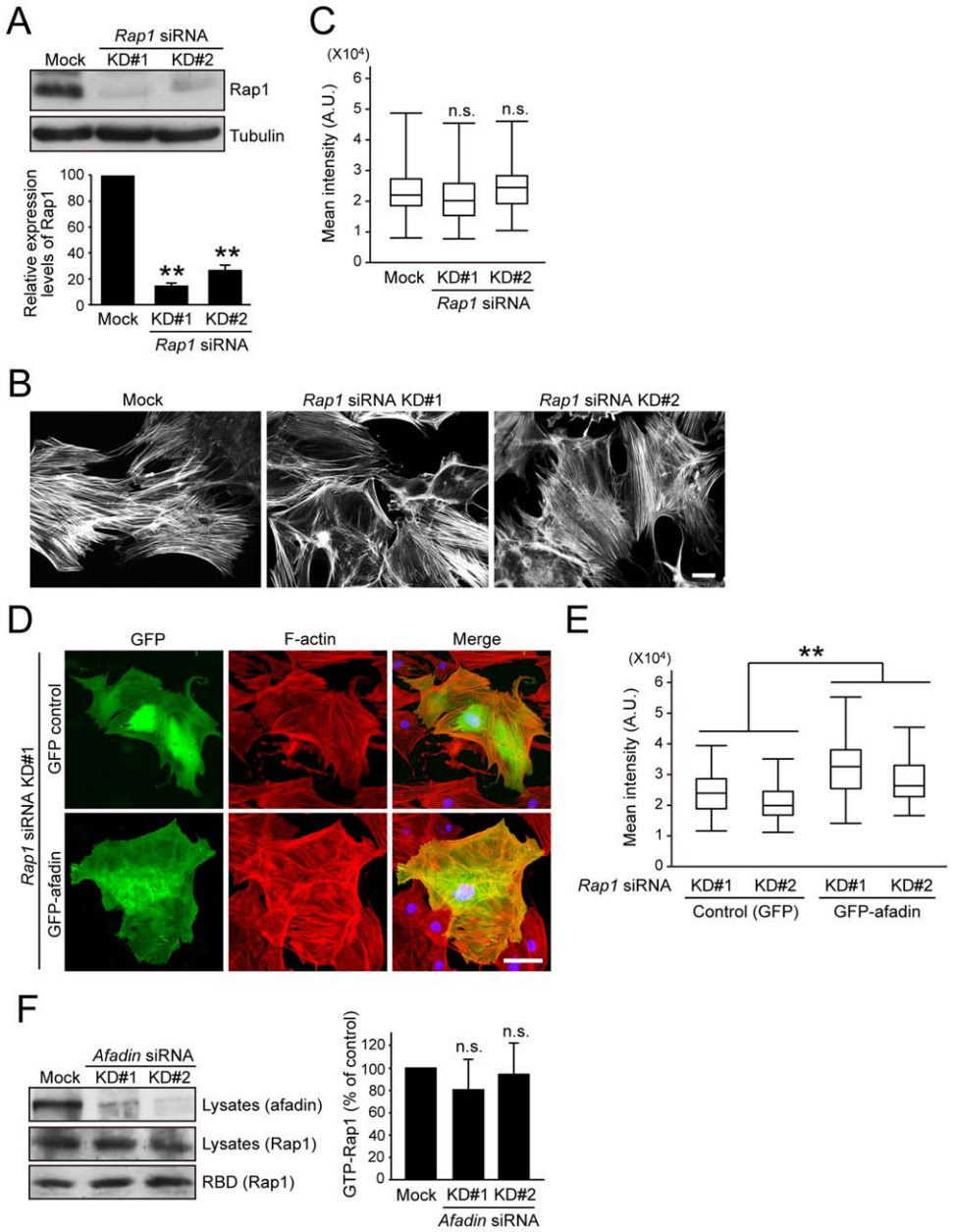

Fig. 6. Afadin regulates actin stress fiber formation in a Rap1-independent manner in C7 cells. A: C7 cells cultured at 33°C were transfected with control (mock) or *Rap1* siRNAs and cultured at 37°C for 7 d. Rap1 and tubulin (loading control) were detected by immunoblotting using anti-Rap1 and anti-tubulin antibodies, respectively. The efficiency of Rap1 depletion by siRNAs was quantified and statistically analyzed as in Fig. 1D (**$P < 0.01$). **B**: Mock and Rap1-depleted cells cultured as in A were fixed and stained with phalloidin for F-actin. Scale bar, 50 μm. **C**: Quantification of stress fiber density of mock and Rap1-depleted cells. The data of more than 100 cells was statistically analyzed as in Fig. 1F (n.s. = not significant). **D**: For cotransfection of plasmid DNA and siRNA, C7 cells cultured at 33°C were first transfected with *Rap1* siRNAs and cultured at 37°C. After 6 d, cells were cotransfected with a control plasmid (pEGFP) or pEGFP plasmid encoding afadin, followed by additional 24 h culture. The cotransfected cells were fixed and stained with anti-GFP antibody (green), phalloidin (red), and hoechst 33258 for nuclei (blue). Merged fluorescent images are shown. Scale bar, 50 μm. **E**: Quantification of stress fiber density of cells transfected as in D. The data of more than 40 transfected cells was analyzed statistically as in Fig. 1F (**$P < 0.01$). **F**: C7 cells were transfected with mock or *afadin* siRNAs and cultured for 7 d. Cell lysates were incubated with GST-RalGDS-RBD that was immobilized on glutathione-Sepharose beads. The amount of Rap1 in cell lysates before pull-down and GTP- (GST-RBD bound) Rap1 was detected by immunoblotting using anti-Rap1 antibody. Depletion of afadin by siRNAs was confirmed by immunoblotting using anti-afadin antibody. The amount of GTP-Rap1 was normalized to that of total Rap1 and expressed as the means ± S.D. of four independent experiments. *P* values in comparison to mock cells as determined by Student's *t*-test are shown (n.s. = not significant). [Color figure can be viewed in the online issue, which is available at wileyonlinelibrary.com.]

UGAU-3' (rat, nt 3906–3930 and mouse, nt 3885–3909); *RhoA*, KD#1 5'-GAAAGACAUGCUUGCUCAUAGUCU U-3' (human, nt 50–74) and KD#2 5'-UGUUUGAGAAC UAUGUGGCAGAUAU-3' (human, nt 113–137); *Rap1*, KD#1 5'-CAGCAAUGAGGGAUUUGUAUAUGAA-3' (rat, nt 194-218) and KD#2 5'-CAGAAUUUAGCAAGA CAGUGGUGUA-3' (rat, nt 394–418). Human *RhoA* siRNAs have a single-base mismatch to the Rat *RhoA* mRNA (underline), but significantly reduced the expression of endogenous RhoA in C7 cells (see Fig. 2A).

Cell Culture and Transfection

Rat kidney podocyte cell line C7 was established as previously described [Eto et al., 2007] and characterized [Chittiprol et al., 2011]. C7 cells were cultured on type I collagen-coated dishes in Dulbecco's modified Eagle's medium/F-12 medium (DMEM/F12, Sigma) supplemented with 5% fetal bovine serum (FBS), 50 U/ml penicillin/streptomycin, and insulin/transferrin/selenium A (Invitrogen) at 33°C (permissive temperature) in 5% CO_2 and passaged for proliferation. For induction of differentiation, C7 cells were transferred to 37°C (nonpermissive temperature). C7 cells cultured at 33°C were transfected with control (mock) or siRNA using Lipofectamine RNAiMAX (Invitrogen) according to the manufacture's reverse transfection protocols, and cultured at 37°C for 7 d. For transfection of plasmid DNA, C7 cells that were cultured at 37°C for 6 d were transfected with relevant plasmids using Lipofectamine 2000 (Invitrogen) according to the manufacture's instructions, followed by additional 24 h culture. Mouse fibroblast NIH3T3 cells and human embryonic kidney HEK293 cells were cultured in DMEM supplemented with 10% FBS and 50 U/ml penicillin/streptomycin at 37°C in 5% CO_2. NIH3T3 cells and HEK293 cells were transfected with siRNA for 48 h and plasmid DNA for 24 h, respectively, using Lipofectamine 2000.

Immunostaining and Immunoblotting

Immunostaining was performed as previously described [Saito et al., 2012]. To quantify stress fiber density of the cells, C7 cells were stained with phalloidin for F-actin. For quantification of F-actin, a line was drawn across the center of cells. The fluorescence intensity of F-actin across the lines in the cells was measured using ImageJ (National Institutes of Health, NIH), and the line profile was generated. In the line profile, the *x*-axis represents distance (pixel) across the cell, and the *y*-axis represents levels of fluorescence intensity. Stress fiber density was quantified by calculating total intensity divided by number of pixels (mean intensity). Images were obtained with fixed acquisition parameters in each experiment. For immunoblotting, cells were solubilized with 1% SDS in Phosphate-buffered saline (PBS) containing protease inhibitor cocktail (Sigma) and 1 mM phenylmethylsulfonyl fluoride (PMSF). Cell lysates were separated by SDS-PAGE and transferred to a polyvinylidene difluoride membrane (Millipore). The membrane was blocked with 5% skim milk in PBST (0.05% Tween 20) and incubated with primary antibodies. The primary antibodies were detected with horseradish peroxidase–conjugated secondary antibodies (Bio-Rad laboratories, Hercules, CA) and an ECL detection kit (Thermo Scientific, Rockford, IL).

Pull-Down Assay

GST-Rhotekin-RBD, GST-PAK1-PBD, and GST-RalGDS-RBD were purified from B21 *E. coli*. Pull-down assay was performed as previously described [Ohta et al., 2006] with minor modifications. Cells were washed with Tris-buffered saline and solubilized in RIPA buffer (20 mM Tris-HCl at pH 7.5, 120 mM NaCl, 1% Triton X-100, 0.1% deoxycholate, 0.1% SDS, 10 mM $MgCl_2$, 1 mM EDTA, 1 mM orthovanadate, 1 mM DTT, and 1 mM PMSF) containing protease inhibitor cocktail. Cell lysates were precleared and incubated with GST-Rhotekin-RBD, GST-PAK1-PBD, or GST-RalGDS-RBD in the presence of glutathione-Sepharose 4B (GE Healthcare BioScience, Uppsala, Sweden) for 20 min (GST-Rhotekin-RBD and GST-PAK1-PBD) or 1 h (GST-RalGDS-RBD) at 4°C. The glutathione-Sepharose beads were washed four times with wash buffer (20 mM Tris-HCl at pH 7.5, 120 mM NaCl, 0.1% Triton X-100, 10 mM $MgCl_2$) and the extent of GTP-bound small GTPases was determined by immunoblotting using anti-RhoA, anti-Rac1, anti-Cdc42, or anti-Rap1 antibody.

Statistical Analysis

The statistical significance was accessed by two-tailed unpaired Student's *t*-test or Mann-Whitney's *U*-test. Differences were considered to be statistically significant at P value of < 0.05. Error bars (S.D.) and P values were determined from results of at least three or more experiments.

Acknowledgments

The authors thank Y. Takai (Kobe University, Japan) for afadin constructs, K. Tamai (Cyclex Co., Japan) for GST-Rhotekin-RBD construct, and K. Katagiri (Kitasato University, Japan) for GST-RalGDS-RBD construct. The authors are grateful for the excellent technical assistance of Kazuko Kurita, Sayuri Aoyama, and Yuka Mochizuki. This work was supported by Grants-in-Aid for Scientific Research from the Japan Society for the Promotion of Science and the Ministry of Education, Culture, Sports, Science, and Technology of Japan, Grant for All Kitasato Project Study, and Kitasato University Research Grant for Young Researchers.

References

Asada M, Irie K, Morimoto K, Yamada A, Ikeda W, Takeuchi M, Takai Y. 2003. ADIP, a novel afadin- and α-actinin-binding protein localized at cell-cell adherens junctions. J Biol Chem 278: 4103–4111.

Asada M, Irie K, Yamada A, Takai Y. 2004. Afadin- and α-actinin-binding protein ADIP directly binds β'-COP, a subunit of the coatmer complex. Biochem Biophys Res Commun 321:350–354.

Asanuma K, Yanagida-Asanuma E, Faul C, Tomino Y, Kim K, Mundel P. 2006. Synaptopondin orchestrates actin organization and cell motility via regulation of RhoA signalling. Nat Cell Biol 8:485–491.

Birukova AA, Tian X, Tian Y, Higginbotham K, Birukov KG. 2013. Rap-afadin axis in control of Rho signaling and endothelial barrier recovery. Mol Biol Cell 24:2678–2688.

Boettner B, Harjes P, Ishimaru S, Heke M, Fan HQ, Qin Y, Van Aelst L, Gaul U. 2003. The AF-6 homolog canoe acts as a Rap1 effector during dorsal closure of the drosophilla embryo. Genetics 165:159–169.

Böhl F, Kruse C, Frank A, Ferring D, Jansen RP. 2000. She2p, a novel RNA-binding protein tethers ASH1 mRNA to the Myo4p myosin motor via She3p. EMBO J 19:5514–5524.

Chittiprol S, Chen P, Petrovic-Djergovic D, Eichler T, Ransom RF. 2011. Marker expression, behaviors, and responses vary in different lines of conditionally immortalized cultured podocytes. Am J Physiol Renal Physiol 301:F660-F671.

Eto N, Wada T, Inagi R, Takano H, Shimizu A, Kato H, Kurihara H, Kawachi H, Shankland SJ, Fujita T, Nangaku M. 2007. Podocyte protection by darbepoetin: preservation of the cytoskeleton and nephrin expression. Kidney Int 72:455–463.

Faul C, Asanuma K, Yanagida-Asanuma E, Kim K, Mundel P. 2007. Actin up: regulation of podocyte structure and function by components of the actin cytoskeleton. Trends Cell Biol 17:428–437.

Fukumoto Y, Kurita S, Takai Y, Ogita H. 2011. Role of scaffold protein afadin dilute domain-interacting protein (ADIP) in platelet-derived growth factor-induced cell movement by activating Rac protein through Vav2 protein. J Biol Chem 286:43537–43548.

Hays T, Ma'ayan A, Clark NR, Tan CM, Teixeira A, Teixeira A, Choi JW, Burdis N, Jung SY, Bajaj AO, O'Malley BW, He JC, Hyink DP, Klotman PE. 2014. protemomics analysis of the nonmuscle myosin heavy chain IIa-enriched actin-myosin complex reveals multiple functions within the podocyte. PLoS ONE 9:e100660.

Hoshino T, Sakisaka T, Baba T, Yamada T, Kimura T, Takai Y. 2005. Regulation of E-cadherin endocytosis by nectin through afadin, Rap1, and p120^{ctn}. J Biol Chem 280:24095–24103.

Ichimura K, Kurihara H, Sakai T. 2003. Actin filament organization of foot processes in rat podocytes. J Histochem Cytochem 51:1589–1600.

Jaffe AB, Hall A. 2005. Rho GTPases: biochemistry and biology. Annu Rev Cell Dev Biol 21:247–269.

Johnstone DB, Zhang J, George B, Léon C, Gachet C, Wong H, Parekh R, Holzman LB. 2011. Podocyte-specific deletion of Myh9 encoding nonmuscle myosin heavy chain 2A predisposes mice to glomerulopathy. Mol Cell Biol 31:2162–2170.

Kistler AD, Altintas MM, Reiser J. 2012. Podocyte GTPases regulate kidney filter dynamics. Kidney Int 81:1053–1055.

Lal MA, Andersson AC, Katayama K, Xiao Z, Nukui M, Hultenby K, Wernerson A, Tryggvason K. Rhophilin-1 is a key regulator of the podocyte cytoskeleton and is essential for glomerular filtration. J Am Soc Nephrol 26:647–662.

Long RM, Gu W, Lorimer E, Singer RH, Chartrand P. 2000. She2p is a novel RNA-binding protein that recruits the Myo4p-She3p complex to ASH1 mRNA. EMBO J 19:6592–6601.

Majima T, Takeuchi K, Sano K, Hirashima M, Zankov DP, Tanaka-Okamoto M, Ishizaki H, Miyoshi J, Ogita H. 2013. An adaptor molecule afadin regulates lymphangiogenesis by modulating RhoA activity in the developing mouse embryo. PLoS One 8:e68134.

Mandai K, Nakanishi H, Satoh A, Obaishi H, Wada H, Nishioka H, Itoh M, Mizoguchi A, Aoki T, Fujimoto T, Matsuda Y, Tsukita S, Takai Y. 1997. Afadin: a novel actin filament-binding protein with one PDZ domain localized at cadherin-based cell-to-cell adherens junction. J Cell Biol 139:517–528.

Miyata M, Rikitake Y, Takahashi M, Nagamatsu Y, Yamauchi Y, Ogita H, Hirata K, Takai Y. 2009. Regulation by afadin of cyclical activation and inactivation of Rap1, Rac1, and RhoA small G proteins at leading edges of moving NIH3T3 cells. J Biol Chem 284:24595–24609.

Mouawad F, Tsui H, Takano T. 2013. Role of Rho-GTPases and their regulatory proteins in glomerular podocyte function. Can J Physiol Pharmacol 91:773–782.

Mundel P, Reiser J. 2010. Proteinuria: an enzymatic disease of the podocyte?. Kidney Int 77:571–580.

Mundel P, Reiser J, Zúñiga Mejía Borja A, Pavenstädt H, Davidson GR, Kriz W, Zeller R. 1997. Rearrangements of the cytoskeleton and cell contacts induce process formation during differentiation of conditionally immortalized mouse podocyte cell lines. Exp Cell Res 236:248–258.

Nakata S, Fujita N, Kitagawa Y, Okamoto R, Ogita H, Takai Y. 2007. Regulation of platelet-derived growth factor receptor activation by afadin through SHP-2: implications for cellular morphology. J Biol Chem 282:37815–37825.

New LA, Martin CE, Jones N. 2014. Advances in slit diaphragm signaling. Curr Opin Nephrol Hypertens 23:420–430.

Ohta Y, Hartwig JH, Stossel TP. 2006. FilGAP, a Rho- and ROCK-regulated GAP for Rac binds filamin a to control actin remodelling. Nat Cell Biol 8:803–814.

Pellegrin S, Mellor H. 2007. Actin stress fibres. J Cell Sci 120: 3491–3499.

Ponting CP. 1995. AF-6/cno: neither a kinesin nor a myosin, but a bit of both. Trends Biochem Sci 20:265–266.

Reiser J, Sever S. 2013. Podocyte biology and pathogenesis of kidney disease. Annu Rev Med 64:357–366.

Saito K, Ozawa Y, Hibino K, Ohta Y. 2012. FilGAP, a Rho/Rho-associated protein kinase-regulated GTPase-activating protein for rac, controls tumor cell migration. Mol Biol Cell 23:4739–4750.

Schlondorff J. 2008. Nephrin AKTs on actin: the slit diaphragm-actin cytoskeleton signaling network expands. Kidney Int 73:524–526.

Singh N, Nainani N, Arora P, Venuto RC. 2009. CKD in MYH9-related disorders. Am J Kidney Dis 54:732–740.

Takai Y, Ikeda W, Ogita H, Rikitake Y. 2008. The immunoglobulin-like cell adhesion molecule nectin and its associated protein afadin. Annu Rev Cell Dev Biol 24:309–342.

Tian D, Jacobo SM, Billing D, Rozkalne A, Gage SD, Anagnostou T, Pavenstädt H, Hsu HH, Schlondorff J, Ramos A, Greka A. 2010. Antagonistic regulation of actin dynamics and cell motility by TRPC5 and TRPC6 channels. Sci Signal 3:ra77.

Tian X, Kim JJ, Monkley SM, Gotoh N, Nandez R, Soda K, Inoue K, Balkin DM, Hassan H, Son SH, Lee Y, Moeckel G, Calderwood DA, Holzman LB, Critchley DR, Zent R, Reiser J, Ishibe S. 2014. Podocyte-associated talin1 is critical for glomerular filtration barrier maintenance. J Clin Invest 124:1098–1113.

Wang L, Ellis MJ, Gomez JA, Eisner W, Fennell W, Howell DN, Ruiz P, Fields TA, Spurney RF. 2012. Mechanisms of the proteinuria induced by Rho GTPases. Kidney Int 81:1075–1085.

Weins A, Schlondorff JS, Nakamura F, Denker BM, Hartwig JH, Stossel TP, Pollak MR. 2007. Disease-associated mutant α-actinin-4 reveals a mechanism for regulation its F-actin-binding affinity. Proc Natl Acad Sci USA 104:16080–16085.

Zhu L, Jiang R, Aoudjit L, Jones N, Takano T. 2011. Activation of RhoA in podocytes induces focal segmental glomerulosclerosis. Kidney Int 22:1621–1630.